MECHANISM OF PULSED SUPERRADIANCE FROM 2p-1s TRANSITIONS IN NEON

A. A. ISAEV and G. G. PETRASH

P. N. Lebedev Physics Institute, U.S.S.R. Academy of Sciences

Submitted October 8, 1968

Zh. Eksp. Teor. Fiz. 56, 1132–1145 (April, 1969)

The pulsed inversion mechanism in transitions of the 2p–1s group in the neon atom, suggested in the literature, is investigated. The analysis is based on known data on the effective cross sections of excitation of neon atom levels by electron impact from the ground state and from 1s levels. The experimental work was performed to investigate superradiance and generation from the neon transitions. The experiments were carried out with tubes of various diameters and a wide range of discharge conditions. Pulsed superradiance and generation were observed from four transitions of the 2s–2p group and from one transition of the 3d–2p group in the infrared region of the spectrum. A new superradiance was observed at $\lambda = 6266$ Å ($2p_5$–$1s_3$ transition). The superradiance power in various lines is studied as a function of neon pressure and pulse transformer voltage. These functions are found to differ significantly between superradiance lines in the visible and infrared regions. The temporal superradiance characteristics are investigated. The obtained results are used to evaluate the possible inversion mechanisms. It is shown that the basic inversion mechanism at the 2p–1s transitions in neon is the stepwise excitation of the 2p levels by electrons via the intermediate resonance level $1s_2$.

INTRODUCTION

PULSED superradiance and generation from a number of transitions of the 2p–1s group were reported in [1-6] at first in neon and then in other inert gases.[1)] The mechanism of inversion formation at these transitions is still not clear. The present work is aimed at a detailed study of superradiance in neon. The special attention to neon is due to the following considerations. The generation and superradiance in neon are known much better than in other inert gases. Furthermore the level and transition characteristics necessary for the analysis of the above processes are relatively better known for neon. This leads us to the expectation that the choice of the specific inversion mechanism can be more readily justified in the case of neon. Finally superradiance in neon is of the greatest practical interest since, in contrast with other inert gases, the corresponding transitions are located in the visible region of the spectrum. We also note that the highest peak power of a gas laser amounting to 190 kW [7,8] in the visible region was obtained in the green line of neon.

1. CHARACTERISTICS OF NEON LEVELS AND POSSIBLE INVERSION MECHANISMS

Figure 1 shows the neon atom level scheme. Of the thirty allowed transitions in the 2p–1s group superradiance and generation were observed in three. The present paper reports on the observation of superradiance from yet another transition. All these transitions are shown by arrows in Fig. 1 and are given in Table I. The duration of generation and superradiance usually does not exceed 30 nsec. Generation and superradiance

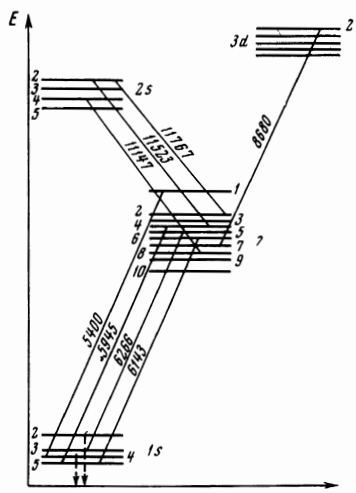

FIG. 1. Diagram of neon levels (Paschen notation). Arrows designate transitions for which pulsed superradiance or generation were observed in our experiments.

are also observed at the beginning of the current pulse. Furthermore a number of workers [1-4,6] reported on superradiance or generation in lines lying in the near infrared. It is noted in [2] that generation in infrared lines begins somewhat earlier than in visible lines. It is not known what transitions were involved in the infrared superradiance.

Table I. Transitions of the 2p–1s group in neon that produced pulsed superradiance or generation

λ, Å	Transition	Reference
5400	$2p_1 - 1s_4$	[2–5,7,8]
5945	$2p_4 - 1s_5$	[1,2,4,5]
6143	$2p_6 - 1s_5$	[1,2,4,5]
6266	$2p_5 - 1s_3$	Present work

[1)] For the sake of brevity we use the Paschen notation here and in the following material. The designations of the investigated neon levels in the LS and *jl* coupling terms are given in Table II below.

Three different points of view were advanced about the mechanism of inversion formation at the 2p–1s transitions. It is assumed in [1,2] that the inversion at the 2p–1s transition is the result of radiative cascades mainly from the 2s levels, and it is considered[1] that stimulated emission from the 2s–2p transitions must be postulated to explain the observed peak power. A mechanism of stepwise excitation of 2p levels by electrons via an intermediate resonant $1s_2$ level is suggested in [4]. A similar point of view was recently stated in [9], based on an analysis of data on the lifetimes and excitation cross sections of neon levels. Finally, it is assumed in [3,7] that the excitation of the upper working level is caused by direct electron impact from the ground state. Which of the three proposed excitation mechanisms plays the controlling role depends in the first place on the relative magnitude of the effective electron excitation cross sections of neon levels.

Table II gives data on the effective cross sections of direct excitation of the relevant levels by electron impact from the ground state of the atom. In the table, the neon levels are designated in LS and jl coupling terms and in the Paschen notation, while the values of effective cross sections at the maximum are given in multiples of 10^{-19} cm^2. The table shows only the results of the most recent work, in which the most complete data were obtained. In particular, the most complete experimental measurements of the cross sections of interest were made in [10,11]. These results are listed in the first and second columns of Table II.

We note that it is very difficult to determine experimentally the effective cross sections of the direct electron excitation of 2p levels since a large number of lines in the infrared must be measured to identify the contribution from cascade transitions. Because of these difficulties cascade transitions were not excluded at all from the results of [10], and were accounted for only partially in [11]. At the same time direct experiments with an electron beam[9,14] provided a definite proof that cascade transitions play an important role in the population of 2p levels mainly from 2s levels. This conclusion is also confirmed by the results of investigating the inversion formation processes in 2s–2p transitions in neon[15–17] and especially by the presence of a continuous and pulsed generation in pure neon under weak currents and low pressures. Incidentally the results reported in [11] also lead to the conclusion that cascade transitions are the principal factor in determining the cross sections measured in that work. In fact the dependence of the measured cross sections from energy, showing a broad maximum and a gentle slope, obtained in [10,11] is typical of allowed transitions, while direct excitation of 2p levels calls for a function with a sharper maximum. For the majority of the 2p levels it was not possible to account for the most important cascades from 2s levels. In the single case of the $2p_{10}$ level, where it was possible to analyze at least partially the cascades from 2s levels, the analysis showed that the measured cross section for the $2p_{10}$ level should be decreased approximately by a factor of three. We also note that according to the available data on the excitation cross sections of the $2s_2$ (see Table II) level and on transition probabilities,[9] the contribution from the cascade transitions to the excitation cross section of 2p levels is comparable in the order of magnitude to the cross section values measured in [10,11]. A comparable contribution can apparently also be expected from the 3d levels.

Consequently the available experimental data on the effective cross sections of direct excitation neon 2p levels should be considered mainly as estimates of the upper limit of the cross section values.

The experimental data on the excitation cross sections of 2s levels were obtained only for the $2s_2$ level in [12]. As far as we know there are no experimental data on the excitation cross sections of 1s levels.

The effective electron excitation cross sections of neon levels were repeatedly calculated theoretically. A recent paper[13] presented the most complete computation of oscillator strengths and effective electron excitation cross sections for many transitions in the neon atom, including all the transitions of interest to us. The computation was performed in the intermediate coupling approximation. The results of this work are also given in Table II.

To compute the effectiveness of the stepwise electron excitation we must also have data on the excitation cross sections of 2p levels from 1s levels.

Experimental measurements of excitation cross section of individual 2p levels excited at once from all 1s levels are reported in [10]. In [18] the same cross sections were measured by a somewhat different method and, in addition, an attempt was made to obtain cross

Table II. Effective cross sections of electron excitation of neon levels from the atomic ground state. Values obtained with partial allowance for cascades from above are given in parentheses

Level			E, eV	Effective cross section in the maximum, 10^{-19} cm^2			
LS	jl	Paschen		no [10]	[11]	[12]	[13]
$3s^1P_1^0$	$3s'\,[1/2]_1^0$	$1s_2$	16.844				28.0
$3s^3P_0^0$	$3s'\,[1/2]_0^0$	$1s_3$	16.723				2.04
$3s^3P_1^0$	$3s\,[1^1/_2]_1^0$	$1s_4$	16.667				3.4
$3s^3P_2^0$	$3s\,[1^1/_2]_2^0$	$1s_5$	16.616				2.6
$3p^1S_0$	$3p'\,[1/2]_0$	$2p_1$	18.961	6.0	38.9		8.58
$3p^3P_1$	$3p'\,[1/2]_1$	$2p_2$	18.734	1.4	5.17		0.03
$3p^3P_0$	$3p\,[1/2]_0$	$2p_3$	18.719	1.1	3.4		0.57
$3p^3P_2$	$3p'\,[1^1/_2]_2$	$2p_4$	18.699	3.2	11 (6.5)		0.18
$3p^1P_1$	$3p'\,[1^1/_2]_1$	$2p_5$	18.689	2.0	5.78		0.005
$3p^1D_2$	$3p\,[1^1/_2]_2$	$2p_6$	18.644	2.9	16 (12.2)		1.8
$3p^3D_1$	$3p\,[1^1/_2]_1$	$2p_7$	18.608	2.3	6.33		0,49
$3p^3D_2$	$3p\,[2^1/_2]_2$	$2p_8$	18.586	3.6	14 (11.2)		0.54
$3p^3D_3$	$3p\,[2^1/_2]_3$	$2p_9$	18.563	2.5	12.4 (8)		1.12
$3p^3S_1$	$3p\,[1/2]_1$	$2p_{10}$	18.317	2.0	11 (5)		2.3
$4s^1P_1^0$	$4s'\,[1/2]_1^0$	$2s_2$	19.69			7.1	1.66
$4s^3P_0^0$	$4s'\,[1/2]_0^0$	$2s_3$	19.67				0.16
$4s^3P_1^0$	$4s\,[1^1/_2]_1^0$	$2s_4$	19.595				2.21
$4s^3P_2^0$	$4s\,[1^1/_2]_2^0$	$2s_5$	19.57				0.30

Table III. Effective cross sections of electron excitation of 2p levels from the $1s_2$ level in neon (10^{-16} cm^2)

Reference	Level									
	$2p_1$	$2p_2$	$2p_3$	$2p_4$	$2p_5$	$2p_6$	$2p_7$	$2p_8$	$2p_9$	$2p_{10}$
[18]	69	17	0	23	21	64	0	14	0	0
[10]*	154	15	0	48	13	33	0	6	0	0
[13]	6,4	8.8	0.88	8.8	16.1	15.0	4.7	6.1	19	8.8

*Effective cross section values obtained from the experimental data in [10] and computed according to [18].

sections of the 2p level excitation from each 1s level separately, assuming that the cross sections are proportional to the corresponding oscillator strengths. The computations reported in [13] and also general considerations indicate that electrons excite the $1s_2$ resonance level much more effectively than the other 1s levels; thus we are mainly interested in the cross sections of excitation of 2p levels from the $1s_2$ level. Table III shows the values of the corresponding cross sections.

Line 1 of the table contains the values of cross sections obtained in [18], and line 2 gives the values obtained on the basis of the experimental data in [10] by a computation similar to that presented in [18]. We note that the values of the corresponding cross sections in the two lines of the table differ on the average by approximately a factor of two which may be regarded as a good agreement, considering the experimental difficulties, the inaccuracy of data in [10], and the fact that under the experimental conditions of [10, 18] the principal contribution to the population of most of the 2p levels came from the $1s_5$ level rather than from the $1s_2$ level. It is noted that the effective cross sections of excitation of 2p levels from the $1s_2$ level obtained from the experiment are fairly large for allowed transitions and reach the order of magnitude of 10^{-15}–10^{-14} cm^2. The last line of Table III contains the values of the corresponding cross sections obtained by computation in [13]. The computed values of these cross sections are somewhat lower and in considerably poorer agreement with the experimental values than the latter have with each other.

A comparison of all the available data leads to the conclusion that the effective cross sections of excitation of 2p levels from the ground state are close in the order of magnitude to 10^{-19} cm^2. The excitation cross sections of the levels $1s_3$, $1s_4$, and $1s_5$ obtained only by computation are of the same order, while the excitation cross section of the $1s_2$ level is considerably larger. The excitation cross sections of levels $2s_2$ and $2s_4$ are somewhat larger than those of 2p levels. From these considerations we can expect pulsed inversion in the leading edge of the excitation pulse in 2s–2p transitions; this indeed is observed in the experiments. An inversion by direct excitation in 2p–1s transitions is hardly possible. Furthermore our evaluation shows that it is possible to obtain pulsed inversion in 2p–1s transitions both by a stimulated cascade from 2s levels and by stepwise electron excitation via the intermediate $1s_2$ level. It is difficult to choose between the cascade and stepwise mechanism on the basis of the available data.

The above conclusions unfortunately cannot be considered sufficiently reliable. It is evident from the above review that the available experimental data on the cross sections are incomplete, fail to reflect the cascade effects to a sufficient degree, and the results of various authors are in marked disagreement. The reliability of the approximations used in the theoretical computations cannot be evaluated. Likewise, the agreement of the computed data with the experimental results cannot be accepted as satisfactory. In this situation it is hardly possible to solve the problem by computing the inversion. Consequently the primary attention in the following discussion is paid to the experimental investigation.

2. EXPERIMENTAL INVESTIGATION OF SUPERRADIANCE AND GENERATION IN NEON

The setup used in our experiments is shown in Fig. 2. Superradiance and generation in neon were studied in three tubes. Two had an active length of 20 cm and internal diameter of 1.3 and 5 mm, while the third had an active length of 120 cm and a diameter of 6.5 mm. All the discharge tubes were made of quartz. Only cold electrodes were used. It was noted that superradiance

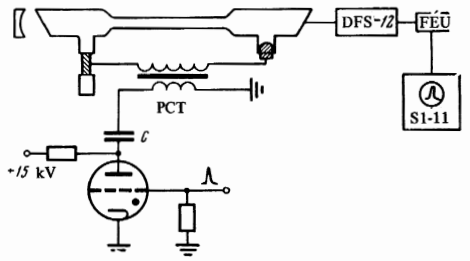

FIG. 2. The experimental setup.

increased considerably when a hollow cylinder was used as the cathode. A hollow kovar cylinder was therefore used as the cathode in the experiments. The anode was represented by a massive tungsten plate of the IFP-2000 tube.

The discharge in the tubes was excited with the aid of a pulse cable transformer (PCT)[19] whose primary was used to discharge a capacitor or a pulse shaping line. We used 0.001, 0.004, and 0.01 μF KVI-3 type capacitors, as well as a special 0.11 μF low-inductance capacitor. In some cases we used a symmetric pulse shaping charging network of cables with a capacitance up to 2500 nF. The results little depended on the excitation method or the capacitance value. The voltage at the PCT primary was varied up to 15 kV. The PCT transformer ratio was approximately 3.5.

The emission of the discharge tube was focused on the slit of a DFS-12 double monochromator with diffraction gratings and was registered by an FÉU-28 photomultiplier for the visible and infrared regions or by an FÉU-36 photomultiplier for the infrared region of the spectrum. From the photomultiplier the signal entered the input of the S1-11 oscilloscope amplifier. The time constant of the entire recording system was 10–15 nsec. The current pulse was measured with a shunt and also by a Rogowski belt operating in the current transformer mode. The Rogowski belt was wound on a small ferrite ring. The current pulse had the form of a damped oscillation with an amplitude up to 100 A. The superradiance power was measured with a calibrated thermopile. The pulse repetition frequency was varied from a few to several hundred Hz.

The emission of the discharge tubes was studied in two modes: in the generation mode, i.e., in the presence of the resonator consisting of two mirrors, or in the superradiance mode, i.e., with only one mirror behind the tube. In most cases occurring under our experimental conditions the intensity of the investigated stimulated emission lines was considerably lower in the presence of two mirrors than in the superradiance mode. Therefore a large part of the results given be-

low was obtained with only one mirror behind the tube. We note, however, that this mirror did not exert a significant effect on the superradiance intensity for all the lines and under all experimental conditions.

The obtained results depended significantly on the diameter of the discharge tube. In the case of a narrow tube 1.3 mm in diameter and 20 cm long superradiance in the visible region was observed in three lines:

λ, Å	Transition	Line
6143.06	$2p_6 - 1s_5$	Strong
5944.8	$2p_4 - 1s_5$	Weak
6266.5±0.1	$2p_5 - 1s_3$	Weak

The wavelength of the newly discovered 6266 Å line was measured by a photographic method using the DFS-13 instrument with a dispersion of 2 Å/mm. Within the limit of this error this line could be attributed only to the $2p_5-1s_3$ transition. The wavelengths of the remaining lines were measured photoelectrically, using the DFS-12 instrument. Neither superradiance nor generation were observed under any experimental conditions in the green line at 5400 Å from the narrow tube. In addition to superradiance in the visible region this tube also produced superradiance in the infrared at the following lines:

λ, Å	Transition	Line
11 523	$2s_2 - 2p_4$	Strong
11 767	$2s_2 - 2p_2$	Strong
11 143	$2s_4 - 2p_8$	Strong
8681	$3d_2 - 2p_7$	Weak

Figure 3a shows the superradiance peak power as a function of neon pressure in a tube 1.3 mm in diameter and 20 cm in active length. The voltage at the PCT primary was 7 kV and the pulse repetition frequency was 100 Hz. There were no resonator mirrors. Curve 1 is plotted for the 6143 Å line and characterizes the behavior of superradiance in the visible region since the 5945 and 6266 Å lines show a similar behavior except for the fact that their peak power is much lower. Curve 2 pertains to the 8681 Å line and curve 3 to the 11 523 Å line; the remaining lines of the 2s–2p group follow the same relationship. According to Fig. 3a, the behavior of superradiance in lines belonging to different transition groups is markedly different. The optimal pressure amounts to 1.3 Torr for lines of the 2p–1s group, 2.4 Torr for the 3d–2p line, and about 5 Torr for the 2s–2p lines.

The installation of a mirror behind the narrow tube increased the superradiance power only in the 6143 and 5945 Å lines. In the 5945 Å the mirror was effective only when set almost directly against the tube. The mirror did not increase the superradiance power at all neon pressures. It was effective in the 6143 Å line only within the pressure range from 0.1 to 1.5 Torr, and in the 5945 Å line in the range from 1 to 2 Torr. At the same time in the case of the 6143 Å line the mirror reduced the optimum pressure to 0.6 Torr. The mirror behind the tube, when it was effective, caused a sharp narrowing of the superradiance spot. Thus under optimal conditions the mirror increased the superradiance intensity in the 6143 Å line approximately 25 times near the spot center, while the total intensity increased 4 times.

A wider tube 5 mm in diameter and 20 cm in active length produced the same superradiance lines as the narrow tube, except for the 6266 Å line. In addition, we observed superradiance and generation in the 5400 Å

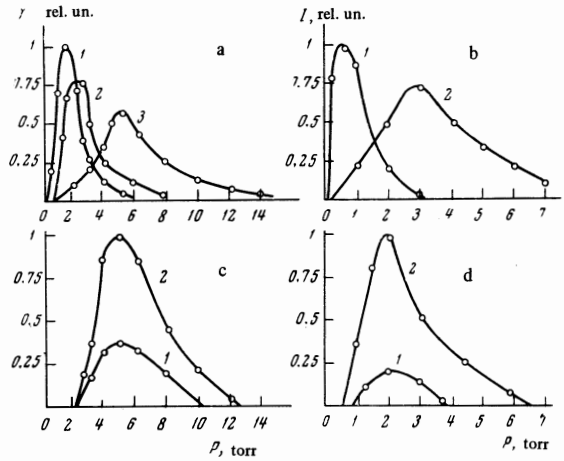

FIG. 3. Peak power of superradiance or generation as a function of neon pressure. a–tube 1.3 mm in diameter and 20 cm long, PCT primary voltage U = 7 kV; curve 1–λ = 6143 Å, 2–λ = 8680 Å, 3–λ = 11 523 Å. b–tube 5 mm in diameter and 20 cm long, U = 7 kV; curve 1–λ = 6143 Å, = 6143 Å, 2–λ = 11 523 Å. c–tube 6.5 mm in diameter and 120 cm long, U = 12 kV, λ = 5400 Å; curve 1–superradiance mode, 2–generation mode. d–tube 6.5 mm in diameter and 120 cm long, U - 12 kV, λ = 11 523 Å; curve 1–generation mode, 2–superradiance mode.

line ($2p_1-1s_4$). In contrast with the 1.3 mm tube the mirror behind the wide tube increased the superradiance intensity in all lines and in all their ranges, except for the 5945 Å line where the mirror had no effect at all. Therefore Fig. 3b shows the superradiance peak power as a function of neon pressure for the case of the mirror placed behind the tube. The PCT voltage was 7 kV and the pulse repetition frequency was 100 Hz. Curve 1 reflects the behavior of superradiance in the visible region in the 6143 and 5945 Å lines. Their optimal pressure was 0.6 Torr. Curve 2 refers to infrared lines of the 2s–2p group. Their optimal pressure is 3 Torr. Generation in the 5400 Å line in this tube exists in the pressure range from 2 to 10 Torr and shows a blurred maximum at about 5 Torr.

A stronger superradiance and generation were observed in the 5400 Å line in a tube 120 cm long and 6.5 mm in diameter. Figure 3c shows the peak power as a function of neon pressure for this line. The PCT voltage was 12 kV and the pulse repetition frequency was 15 Hz. Curve 1 was plotted in the superradiance mode, and curve 2 in the generation mode. The optimal pressure was ~5 Torr. We used spherical mirrors with a radius of curvature of 2 m and aluminum coating. One mirror had no transmission while that of the other was 10–15%. According to the graph, the generation mode yields a large power in such a case. Neither superradiance nor generation were observed in other lines of the visible region from the tube 120 cm long and 6.5 mm in diameter. In the infrared region the same superradiance lines were observed as in the other tubes. The peak power of the infrared lines as a function of pressure is given in Fig. 3d where curve 1 corresponds to the generation mode and curve 2 to the superradiance mode. The experimental conditions are the same as in the case of the 5400 Å line.

The behavior of superradiance lines belonging to various transition groups, depending on PCT voltage or

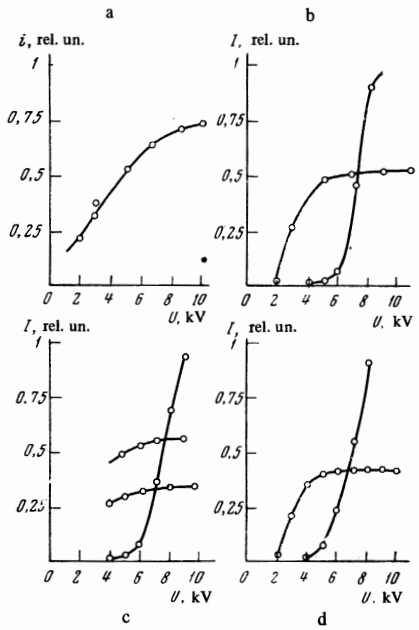

FIG. 4. Current amplitude i_{max} and peak superradiance power I as functions of PCT primary voltage. a–i_{max}, tube 5 mm in diameter and 20 cm long, neon pressure 0.7 torr; b–peak superradiance power I, tube 1.3 mm in diameter and 20 cm long, neon pressure 2.3 torr; c–I, tube 5 mm in diameter and 20 cm long, neon pressure 0.2 torr; d–I, tube 5 mm in diameter and 20 cm long, neon pressure 0.2 torr. Single mirror behind the tube was used in all cases.

discharge current, was also found to differ. Figure 4a shows the current pulse amplitude as a function of PCT primary voltage for the tube 5 mm in diameter and 20 cm long. The neon pressure amounted to 0.7 Torr. According to the graph, with increasing voltage the discharge current first increases linearly and then rises more slowly. Figure 4b shows the dependence of the superradiance peak power on the voltage of PCT primary for a narrow tube 1.3 mm in diameter and 20 cm long. The neon pressure was 2.3 Torr in this case. Figures 4c and 4d show analogous dependencies for a tube 5 mm in diameter and 20 cm long. The neon pressure was 0.7 Torr in Fig. 4c and 0.2 Torr in Fig. 4d. The steeply increasing curves in Figs 4b–d represent the 6143 Å line and the curves with saturation represent the 11 523 Å line. In addition Fig. 4c shows a curve for the 11 143 Å line (bottom). All the curves were obtained with one mirror set behind the tube. According to the graphs superradiance in infrared lines begins with considerably lower voltages and currents than superradiance from 2p–1s transitions. The steep rise of superradiance power from 2p–1s transitions begins only with the onset of power saturation in lines of the 2s–2p group. When PCT primary voltage was boosted to 10–15 kV saturation was also observed at 2p–1s transitions.

Oscilloscopic recording of the superradiance pulses in various lines showed that the duration of superradiance in all lines weakly depended on the experimental conditions and amounted to 10–15 nsec. The duration of generation in the 5400 Å line was about 20 nsec in the tube 5 mm in diameter and 20 cm long. However we must note that the time constant of our equipment was estimated at ~10–15 nsec. It is possible that a better time resolution will help reveal additional details. Within the above accuracy limits, superradiance in all lines occurred practically simultaneously. The oscilloscopic traces of superradiance in the 6143 Å line from the narrow tube 1.3 mm in diameter and 20 cm long had a special feature. Two traces are shown in Fig. 5 for this case. Curve 1 corresponds to an unattenuated light signal, and curve 2 was plotted with the light signal attenuated approximately 10^3 times by gray filters. The high peak in curve 1 is strongly distorted by a nonlinearity of the recording system. According to the graph two superradiance maxima separated in time by approximately 20 nsec are present. The amplitude of the first peak is approximately 10^3 times lower than that of the second peak. This effect was not observed in other lines and in the same line from other tubes.

The power of superradiance was measured with a calibrated thermopile. The average power was about 2 μW under a pressure in the narrow tube that was optimal for the 6143 Å and with a pulse repetition frequency of 50 Hz. This corresponds to a peak power of

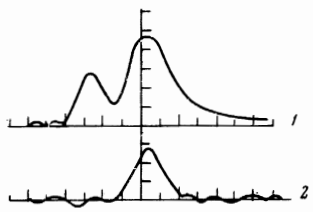

FIG. 5. Oscilloscopic traces of superradiance pulse in the 6143 Å line in a tube 1.3 mm in diameter and 20 cm long. PCT voltage U = 7 kV, neon pressure 0.6 torr. 1–unattenuated signal, large peak distorted by nonlinear recording circuit; 2–light signal attenuated 10^3 times by gray filters.

4 W and power density of 13 W/cm^3 for a pulse length of 10 nsec. In the tube 5 mm in diameter and 20 cm long the peak power of superradiance was 5 W and energy density was 1.25 W/cm^3. Superradiance lines in the infrared region had peak power of ~2 W for the same pressure in the tube 5 mm in diameter and 20 cm long.

3. DISCUSSION OF RESULTS

The above experimental results allow us to form a definite idea on the mechanism of formation of pulse inversion at 2p–1s transitions in neon. We first note that the mechanism of cascade population of the upper levels proposed in [1,2] is not in agreement with experimental data. Cascade population of 2p levels, as pointed out above, mainly proceeds from 2s levels and apparently to a lesser degree from the 3d levels. Direct electron impact from 2s levels effectively populates two levels: $2s_2$ and $2s_4$ which are optically connected with the ground state. Under our experimental conditions we observed superradiance from these levels to some of the 2p levels. We also observed superradiance from the $3d_2$ level. The fact that under many conditions the mirror behind the tube failed to increase the superradiance intensity shows that the corresponding transitions were close to saturation. This means that levels $2s_2$, $2s_4$, and $3d_2$ were almost completely decayed by the transitions that gave rise to superradiance. Un-

der these conditions the rate of cascade population of those 2p levels that terminate the superradiance lines is obviously much higher than that of other levels of the 2p group because the contribution from spontaneous cascades from levels other than 2s and 3d is relatively small. Thus it is sufficient to consider only the stimulated cascades. According to Fig. 1 and Table I the infrared superradiance from levels 2s and 3d terminates at levels $2p_2$, $2p_4$, $2p_7$, and $2p_8$, while the superradiance in the visible region begins with levels $2p_1$, $2p_4$, $2p_5$, and $2p_6$. Consequently three of four superradiance lines at the 2p–1s transitions cannot be explained by radiative cascades at all.

The 5945 Å line ($2p_4$–$1s_5$) requires a separate analysis. The inversion at this transition can be due to cascade pumping at the expense of superradiance in the 11 523 Å line ($2s_2$–$2p_4$). However the absence of exact correlation between these two lines indicates that cascade population is also not the primary inversion cause in the case of the 5945 Å line. In particular, as we see from Fig. 3, the pressure-dependent superradiance powers are markedly different in the infrared and visible lines and fail to exhibit any correlation. At the same time it is typical of cascade correlation that the power peak in one line of the cascade also shows a peak in the other cascade line for the same pressure.[20, 21] Voltage-dependent superradiance powers are also different in infrared and visible lines (see Fig. 4). Likewise, no similarity in the behavior of visible and infrared superradiance lines is observed in the effect of the mirror. Consequently the sum of experimental data leads us to the conclusion that the population of 2p levels by radiative cascade from above fails to exert a noticeable effect on the formation of pulsed inversion at the 2p–1s transitions in neon.

We are now left with the choice between the direct and stepwise population of the upper working levels by electron impact. Under our experimental conditions in the presence of strong superradiance from the 2s–2p transitions, i.e., close to saturation, we can regard the pumping rate of those 2p levels that terminate strong superradiance lines to be practically the same as the pumping rate of the $2s_2$ level. As we pointed out above however, cascade superradiance cannot be realized by experiment. Thus the rate of pumping by direct electron impact with an effective cross section of about 7×10^{-19} cm^2 (excitation cross section of the $2s_2$ level) is insufficient to obtain inversion at the 2p–1s levels. The above data on effective cross sections of direct excitation of neon levels from the atomic ground state (if we note that experimental data yield elevated values because cascades are not taken into account) show that the excitation cross section of the $2s_2$ level is greater than that of 2p levels. This is also convincingly shown by the presence of pulsed and continuous generation and superradiance from 2s–2p transitions. Therefore, if inversion at 2p–1s transitions cannot be achieved by stimulated cascade pumping it is, in general, even less probable by direct electron excitation of 2p levels.

We also should note that, assuming the population of 2p levels by a direct electron impact, the ratio of population rates of levels 2s and 2p does not change with changing electron density since the population of levels $2s_2$ and $2s_4$ proceeds by direct electron impact according to all available data. In this case the behavior of infrared and visible superradiance lines would become similar with varying current. However the experiment shows a noticeable difference in the behavior of these lines (see Fig. 4). Here the superradiance from 2p–1s transitions appears with larger currents than does the infrared superradiance and grows faster with increasing current. At the same time the probabilities of 2p–1s transitions are approximately by an order higher than those of 2s–2p transitions. This means that superradiance from 2p–1s transitions should appear with lower currents than in the case of the 2s–2p transitions for a comparable pulsed pumping rate. Therefore the experimentally observable facts are in disagreement with the mechanism of direct electron excitation of 2p levels.

On the other hand it is well known[9, 10, 15, 18] that the population of 2p levels in neon is to a considerable extent due to the stepwise excitation from 1s levels even at low current densities. It is therefore appropriate to ascribe the inversion at 2p–1s levels to stepwise electron excitation of 2p levels.[4] Since superradiance from 2p–1s transitions appears at the beginning of the current pulse, we are interested in the neon level population processes that occur precisely at that time. With a moderate pulse repetition frequency, such as that used in our experiments, all neon atoms are in the ground state before the start of each current pulse. It follows from general considerations and also from the data in Table II that at the beginning of the current pulse the $1s_2$ resonance level is populated from the ground state faster than others. The large population of the $1s_2$ level is also indicated by the fact that neither neon nor other inert gases show superradiance or generation that terminates at the $1s_2$ level. The effective excitation cross sections of 2p levels from the $1s_2$ level are very large, of the order of 10^{-15} cm^2 (see Table III). Furthermore, under conditions typical of the pulsed discharge in neon, the average electron energy in the discharge seems to be close to the energy corresponding to the maximum of the excitation cross section at 1s–2p transitions. Consequently, the effectiveness of stepwise population of 2p levels via the $1s_2$ resonance level is extremely high.

Table III clearly shows that the highest rate of stepwise excitation is reached at levels $2p_1$, $2p_4$, $2p_5$, and $2p_6$, i.e., precisely at those levels that produce superradiance and generation. The rate of stepwise excitation by electrons, in contrast to the direct excitation, is proportional to the square rather than to the first power of electron density. This means that pulsed inversion at the 2p–1s transitions should be obtained most successfully in rapid discharge at high current densities, and this is actually observed in experiments. On the other hand pulsed generation from 2s–2p transitions due to direct excitation of 2s levels is observed at relatively weak excitation.[16] Furthermore inversion from stepwise excitation should be delayed in time somewhat in comparison to inversion from direct population. In accordance with this consideration infrared superradiance was observed in [2] 8 nsec earlier than the visible superradiance. The insufficient time resolution of our equipment prevented us from proving the existence of such a shift.

We now consider the lines that can be expected to

Table IV. Wavelengths and $\lambda^3 A_{ik}$ factors for allowed transitions $2p_i - 1s_{3-5}$ *

	$1s_5$		$1s_4$		$1s_3$		$1s_2$	
	λ, Å	$\lambda^3 A_{ik}$, rel. un.	λ, Å	$\lambda^3 A_{ik}$, rel. un.	λ, Å	$\lambda^3 A_{ik}$, rel. un.	λ, Å	Q, 10^{-16} cm^2
$2p_1$			**5400**	**11**			5852	69
$2p_2$	5882	167	6029	105	6163	358	6599	17
$2p_3$			6074	1255			6652	0
$2p_4$	**5945**	**190**	6096	354			6678	23
$2p_5$	5975	66	6128	11,5	**6266**	**558**	6717	21
$2p_6$	**6143**	**535**	6305	113			6929	64
$2p_7$	6217	125	6383	787	6533	330	7024	0
$2p_8$	6334	417	6506	795			7174	14
$2p_9$	6402	1350						0
$2p_{10}$	7032	850	7245	385	7439	128	8082	0

*For $2p_i - 1s_2$ transitions the values of effective excitation cross sections Q from the $1s_2$ level are given according to [18].

produce superradiance according to the stepwise excitation theory. It is clear that superradiance is first observed from transitions with the highest gain. The gain at the line maximum is written in the form

$$K = \frac{\lambda^2}{4} \frac{A_{ik}}{\Delta\omega} \left(N_i - \frac{g_i}{g_k} N_k \right),$$

where λ is the wavelength at the $i \rightarrow k$ transition, A_{ik} is the transition probability, $\Delta\omega$ is the line width in angular frequency terms, N_i and N_k are populations of the upper and lower levels, and g_i and g_k are statistical weights of the levels. For a Doppler broadening of the lines $K \sim \lambda^3 A_{ik}$.

Table IV shows wavelengths and the magnitudes of $\lambda^3 A_{ik}$ for all the allowed transitions from 2p levels to the levels $1s_{3,4,5}$. The values of A_{ik} are taken from [9]. Obviously there can be no superradiance terminating at the $1s_2$ level in our system. Therefore the column for $2p-1s_2$ transitions cites figures for the cross sections of excitation of 2p levels from the $1s_2$ level taken from [18]. The table shows in boldface figures for transitions that produced superradiance and generation. The figures of the last column show that levels $2p_1$, $2p_4$, $2p_5$, and $2p_6$ should be populated most of all. Superradiance at these levels should be observed from transition with the higher gain. Consequently superradiance at levels $2p_6$ and $2p_5$ is observed from transitions for which the quantity $\lambda^3 A_{ik}$ has the highest value. At the $2p_4$ level superradiance is observed from a transition for which the quantity $\lambda^3 A_{ik}$ is not the highest. This seems to be due to the fact that the transition $2p_4 - 1s_4$ with a higher $\lambda^3 A_{ik}$ terminates at a level that is optically coupled to the ground state and that can therefore take a greater electron population.

The 5400 Å line ($2p_1 - 1s_4$) calls for a separate analysis since its behavior is markedly different from that of the remaining lines. This line was observed in wider tubes and under higher neon pressures. Its gain is noticeably lower than that of other lines. In contrast to the other lines, it yields larger power in the generation mode. According to Fig. 4 stepwise excitation from the $2p_1$ level can result in only one generation line at 5400 Å. The value of $\lambda^3 A_{ik}$ is for this line by an order lower than for other lines capable of superradiance. In this connection the gain of this line is considerably lower for a comparable pumping rate. Furthermore the $2p_1$ level decays to the $1s_2$ level with a much higher probability than to the $1s_4$ level.[9] Therefore effective inversion at the $2p_1 - 1s_4$ transition requires emission trapping at the pumping transition $1s_2 - 2p_1$ that is achieved at high pressures and large diameters of the discharge tubes.

Thus only the mechanism of stepwise excitation of the 2p levels by electrons via the $1s_2$ resonance level can serve as an explanation of superradiance and generation at the 2p–1s transitions in neon observed in the experiments.

In conclusion we note that stepwise electron excitation can be effective in creating inversion at transitions whose upper level is optically coupled to the resonance level rather than to the ground level. With high electron densities and sufficiently large cross sections of excitation from the resonance level the excitation rate can be comparable to that achieved by direct excitation at an allowed transition. The necessary electron densities are readily achievable in pulsed discharges. This permits us to expect an inversion at many transitions for which direct excitation fails. For example stepwise excitation of mercury can lead to pulsed inversion at the $7^3S_1 - 6^3P_{2,0}$ transitions by pumping via the triplet resonance level. Experiments are underway to achieve this generation. Similar possibilities exist in relation to other atoms.

The authors express their sincere thanks to L. A. Vaĭnshteĭn and L. A. Minaeva for the discussion of theoretical data on the effective excitation cross sections of neon, and to V. M. Kaslin and A. S. Nasibov for valuable discussion of the experiment.

[1] D. Rosenberger, Phys. Lett. **13**, 288 (1964).
[2] D. M. Clunie, R. S. A. Thorn, and K. E. Trezise, Phys. Lett. **14**, 28 (1965).
[3] D. A. Leonard, R. A. Neal, and E. T. Gerry, Appl. Phys. Lett. **7**, 175 (1965).
[4] I. N. Knyazev and G. G. Petrash, Zh. Prikl. Spektr. **4**, 560 (1966).
[5] A. A. Isaev and G. G. Petrash, Elektronnaya Tekhnika, seriya 3, Gazorazryadnye Pribory (Electronics Engineering, Series 3, Gas Discharge Devices) **3**, 17 (1967).
[6] D. Rosenberger, Phys. Lett. **14**, 32 (1965).
[7] D. A. Leonard, IEEE J. Quantum Electronics **QE-3**, 133 (1967).

[8] J. Shipman, Appl. Phys. Lett. **10**, 3 (1967).
[9] W. R. Bennett and P. J. Kindlman, Phys. Rev. **149**, 38 (1966).
[10] S. E. Frish and V. F. Reval'd, Opt. Spektrosk. **15**, 726 (1963).
[11] P. V. Fel'tsan, Author's Abstract of Candidate's Thesis, Kiev, 1967; I. P. Zapesochnyĭ, P. V. Fel' tsan, and M. M. Povch, Ukr. Fiz. Zh. **11**, 232 (1967).
[12] P. K. Tien, D. McNair, and H. L. Hodges, Phys. Rev. Lett. **12**, 30 (1964).
[13] L. A. Vaĭnshteĭn and L. A. Minaeva, FIAN Preprint, 1966.
[14] W. R. Bennett, Adv. in Quantum Electronics, J. Singer, Ed., Columbia University Press, 1961, p. 28.
[15] W. R. Bennett, Appl. Optics, Suppl. No. 1 on Optical Masers, 1962.
[16] G. G. Petrash and I. N. Knyazev, Zh. Eksp. Teor. Fiz. **45**, 832 (1963) [Sov. Phys.-JETP **18**, 571 (1964)].
[17] C. K. N. Patel, J. Appl. Phys. **33**, 3194 (1962).
[18] I. M. Veterov and V. P. Chebotaev, Opt. Spektrosk. **23**, 854 (1968).
[19] A. S. Nasibov, A. A. Isaev, V. M. Kaslin, and G. G. Petrash, Pribory i Tekhn. Eksp. No. 4, 232 (1967).
[20] R. der Agobian, J. L. Otto, R. Cagnard, and R. Echard, Compt. rend. **259**, 85 (1964).
[21] O. Andrade, M. Gallardo, and K. Bockasten, Appl. Phys. Lett. **11**, 99 (1967).

Translated by S. Kassel
130